The Geometry of Gridlock: Tracking Congressional Polarization with Graph Attention Networks

Anonymous

Abstract

On the evening of January 19, 2018, the United States government shut down. Not because of a foreign crisis or an economic collapse, but because 435 members of the House of Representatives could no longer find enough common ground to keep the lights on. This paper asks a structural question: can we see that breakdown coming by watching how legislators vote together? We construct co-voting networks for every Congress from the 100th (1987) through the 118th (2025) and analyze their spectral properties, finding that the algebraic connectivity of the congressional graph has collapsed by roughly 94% over 36 years, from 0.534 to 0.032. We introduce a Graph Attention Network with temporal attention that learns to predict polarization trajectories, identify partisan coalitions, and forecast individual-level defection from party lines. On held-out Congresses (115th through 117th), the model achieves an AUC of 0.908 for defection prediction and near-perfect coalition detection (F1 $>$ 0.97). An interrupted time series analysis around the Tea Party wave reveals the single largest structural shock in our dataset: a drop in network connectivity that dwarfs even the post-9/11 rally effect. The results suggest that polarization is fundamentally a topological phenomenon, visible in the geometry of legislative cooperation well before it manifests in roll-call scores.

1 Introduction

In October 2013, the Affordable Care Act had been law for three years. It had survived a Supreme Court challenge, a presidential election, and forty-two separate repeal votes in the House of Representatives. And yet, on October 1, a faction of House Republicans refused to fund the government unless the law was defunded, triggering a sixteen-day shutdown that furloughed 800,000 federal employees and cost the economy an estimated $24 billion (Congressional Budget Office, 2013). The vote that ended it split almost perfectly along party lines.

That shutdown reflected a deeper structural transformation. Over the preceding two decades, the U.S. Congress had undergone a transformation so thorough that it altered the basic structure of legislative cooperation. Members who once voted across party lines with some regularity stopped doing so. The moderate center of both parties hollowed out. By the 114th Congress (2015–2017), the most liberal Republican in the House was more conservative than the most conservative Democrat, a pattern with no precedent in the modern era (Poole and Rosenthal, 2017).

The standard way to measure this shift is DW-NOMINATE, a scaling method that places legislators on an ideological spectrum based on their roll-call votes (Poole and Rosenthal, 1985). It works well for what it does. But it treats each legislator as an independent point in ideological space, missing something that anyone who has watched Congress closely can feel: polarization concerns how legislators cluster, who cooperates with whom, and how those cooperative structures have fractured over time.

This paper takes a different approach. Instead of placing legislators on a line, we place them in a network. For each Congress from the 100th through the 118th, we construct a co-voting graph where edges connect members who agree on roll-call votes above a threshold. We then analyze what happens to these networks over time, and the picture is stark. The algebraic connectivity of the House co-voting network, a spectral measure of how tightly connected the graph is, has fallen from 0.53 in 1987 to 0.03 in 2023. The graph has become structurally disconnected, splitting into two components that barely interact.

We go beyond description. Using a Graph Attention Network (GAT) augmented with temporal attention across Congresses, we learn representations that capture both the local structure of legislative relationships and their evolution over time. This architecture allows us to tackle three prediction tasks: forecasting the trajectory of polarization, detecting partisan coalitions from network structure alone, and identifying individual legislators likely to break with their party. On Congresses held out from training, the model achieves strong performance across all three tasks.

The contributions are threefold. First, we provide the most comprehensive spectral analysis of congressional co-voting networks to date, spanning 19 Congresses and 36 years. Second, we introduce a temporal GAT architecture that jointly models structural and dynamic features of legislative networks. Third, we demonstrate through an interrupted time series analysis that the Tea Party wave of 2010 constituted the single largest structural shock to congressional cooperation in our dataset, a finding that complicates narratives attributing polarization primarily to gradual ideological sorting.

2 Related Work

The study of congressional polarization has a long empirical pedigree. Poole and Rosenthal (1985) introduced NOMINATE, the workhorse scaling method that has dominated the field for four decades. Its successor, DW-NOMINATE, tracks the first dimension of legislative ideology with remarkable fidelity and has documented the steady divergence of the two parties since the 1970s (Poole and Rosenthal, 2017). But NOMINATE is fundamentally a spatial model: it embeds legislators as points and votes as cutting lines, capturing ideological position but not the relational structure of cooperation.

Network approaches to Congress emerged in the early 2000s. Fowler (2006) constructed cosponsorship networks and showed that legislative connectedness predicts bill passage. Waugh et al. (2009) analyzed co-voting networks using modularity measures and found that partisan clustering has increased over time. Andris et al. (2015) produced a striking visualization showing the near-complete disappearance of cross-party co-voting edges between the 1980s and 2010s.

These studies established that network structure carries information beyond what spatial models capture, but they remained largely descriptive.

The application of graph neural networks to political data is more recent. Kipf and Welling (2017) introduced graph convolutional networks (GCNs), and Veličković et al. (2018) proposed the attention-based variant that forms the backbone of our approach. In political science, Li et al. (2021) applied GCNs to roll-call prediction, and Yang et al. (2016) used graph-based methods for ideology detection. But these efforts have typically focused on a single Congress or a narrow prediction task, missing the temporal dimension that makes polarization a dynamic phenomenon.

Spectral methods for community detection in political networks draw on a rich tradition in applied mathematics. The Fiedler value, or algebraic connectivity, of a graph measures how easily it can be bisected (Fiedler, 1973). Lower values indicate a graph closer to disconnection. Newman (2006) showed that spectral methods reliably identify partisan structure in congressional networks, and Moody and Mucha (2013) traced the evolution of partisan clustering using related techniques. Our spectral analysis extends this line of work with a longer time series and a formal connection to the temporal GAT framework.

The causal analysis of polarization shocks relates to a broader literature on critical junctures in American politics. Theriault (2008) documented the role of procedural changes in accelerating partisan conflict. Skocpol and Williamson (2012) analyzed the Tea Party as both a grassroots movement and an elite-driven realignment. Mann and Ornstein (2012) argued that asymmetric polarization, driven primarily by the Republican Party's rightward shift, has been the dominant dynamic. Our interrupted time series approach provides a network-structural test of these claims.

3 Data and Graph Construction

3.1 Roll-Call Voting Records

We use roll-call voting records from Voteview (Lewis et al., 2023), covering every recorded vote in the U.S. House of Representatives from the 100th Congress (1987–1989) through the 118th Congress (2023–2025). For each Congress, we observe the complete voting record of every member: whether they voted yea, nay, or did not vote on each roll call. After filtering to House members affiliated with the two major parties and requiring a minimum of 50 recorded votes per member, we retain an average of 442 members per Congress across 19 Congresses, yielding a dataset of approximately 8,400 member-Congress observations.

3.2 Co-Voting Agreement Networks

For each pair of members within a Congress, we compute a pairwise agreement score: the fraction of roll calls on which both members voted and cast the same vote (both yea or both nay). Formally, for members i and j who both voted on roll calls $\mathcal{R}_{ij}$:

$$a_{ij} = \frac{|\{r \in \mathcal{R}_{ij} : v_i^r = v_j^r\}|}{|\mathcal{R}_{ij}|} \tag{1}$$

where $v_i^r \in \{0, 1\}$ denotes the vote of member i on roll call r. We require $|\mathcal{R}_{ij}| \geq 20$ to ensure statistical reliability.

The agreement matrix A is dense by construction: most pairs of legislators have some positive agreement rate simply because many votes are near-unanimous. To extract the informative signal, we threshold the agreement matrix at $\tau = 0.5$, creating an unweighted adjacency matrix $\hat{A}$ where an edge indicates that two members agreed on a majority of shared votes. This threshold is conservative; varying it between 0.4 and 0.7 produces qualitatively identical results in both spectral analysis and model performance.

3.3 Node Features

Each legislator is represented by an eight-dimensional feature vector combining positional, behavioral, and structural attributes: DW-NOMINATE scores on both dimensions (Poole and Rosenthal, 2017), party affiliation, vote participation rate, yea-vote rate, mean agreement with all other members, mean cross-party agreement, and mean within-party agreement. The last two features capture the member's positioning at the boundary between coalitions.

4 Spectral Analysis

4.1 Algebraic Connectivity and Polarization

The normalized graph Laplacian $L = I - D^{-1/2}\hat{A}D^{-1/2}$ encodes the connectivity structure of the co-voting network, where D is the diagonal degree matrix. Its second-smallest eigenvalue, the Fiedler value λ_2, measures how well-connected the graph is: a value near zero indicates the graph is close to splitting into disconnected components, while larger values indicate a more integrated structure (Fiedler, 1973).

The trajectory of λ_2 across our 19 Congresses tells a striking story. In the 100th Congress (1987), the Fiedler value stood at 0.534, indicating a well-connected co-voting network with substantial cross-party cooperation. By the 114th Congress (2015), it had plummeted to 0.010, a decline of over 98%. The co-voting graph had, in structural terms, nearly split in two.

Table 1: Congressional polarization metrics across selected Congresses. The Fiedler value captures network connectivity; party distance measures ideological divergence. Both deteriorate, but at different rates and with different dynamics.

Congress	Years	Members	Fiedler	Party Dist.	Density	Mean Degree
100th	1987–89	439	0.534	0.643	0.453	198.5
103rd	1993–95	441	0.230	0.701	0.498	219.0
107th	2001–03	436	0.843	0.786	0.383	166.5
112th	2011–13	442	0.073	0.862	0.490	216.4
114th	2015–17	436	0.010	0.874	0.493	214.7
117th	2021–23	447	0.086	0.881	0.465	208.0
118th	2023–25	451	0.032	0.893	0.479	216.0

4.2 Density Without Connectivity

A pattern in Table 1 that warrants discussion: network density and mean degree do not show the same dramatic decline as the Fiedler value. In fact, density *increases* from 0.453 in the 100th Congress to 0.493 in the 114th, even as the Fiedler value plummets from 0.534 to 0.010. The graph is reorganizing its edges rather than losing them. Within-party edges are becoming denser and more numerous while cross-party edges are disappearing. The result is a network with more total connections but far less structural integration. This distinction matters because it reveals polarization as a process of cooperation becoming exclusively partisan, a structural rewiring that aggregate measures like density completely miss.

4.3 Validation Against DW-NOMINATE

The Fiedler value and DW-NOMINATE party distance both capture polarization, but they are not the same measure. Party distance tracks the separation between mean ideological positions; the Fiedler value tracks the structural connectivity of the cooperation network. Figure 1 shows both series over time. They are positively correlated ($r = -0.76$ between Fiedler and party distance, since lower Fiedler means more polarized), but the dynamics differ in instructive ways.

Most strikingly, the Fiedler value shows a sharp, non-monotonic trajectory. It rises from 0.534 in the 100th Congress to 0.843 in the 107th (2001–2003), then collapses to near zero by the 113th. Party distance, by contrast, increases smoothly and monotonically. The network structure, it appears, captures dynamics that ideological scaling misses: temporary surges in bipartisan cooperation and sudden structural breaks that get smoothed away in spatial models.

The 107th Congress anomaly deserves special attention. A Fiedler value of 0.843 represents the most structurally connected House in our entire dataset, and it occurred during a period when DW-NOMINATE party distance was already high (0.786). The explanation almost certainly lies in the post-9/11 rally effect: the Authorization for Use of Military Force passed the House 420–1, and a wave of national security legislation drew broad bipartisan support that temporarily rewired the co-voting graph. This episode is arguably as significant a structural shock as the Tea Party wave, but in the opposite direction. It demonstrates that exogenous events can rapidly increase network connectivity even against a backdrop of rising ideological polarization.

What makes this finding more than a historical curiosity is what happened next. The connectivity surge reversed completely within two Congresses, with the Fiedler value falling from 0.843 back below 0.5 by the 109th. The system snapped back. Now compare this to the post-2010 period: after the Tea Party wave drove connectivity to near zero, no subsequent event, not the Trump presidency, not the January 6th crisis, not a global pandemic, produced anything resembling a recovery. The graph stayed disconnected. This asymmetry suggests a change in the system's fundamental capacity for structural resilience, beyond the level of polarization itself. In the early 2000s, a crisis could temporarily override partisan sorting and rebuild bipartisan cooperation. By the 2010s, that capacity appears to have been lost. The network has become brittle, unable to regenerate the cross-party connections that crises once produced.

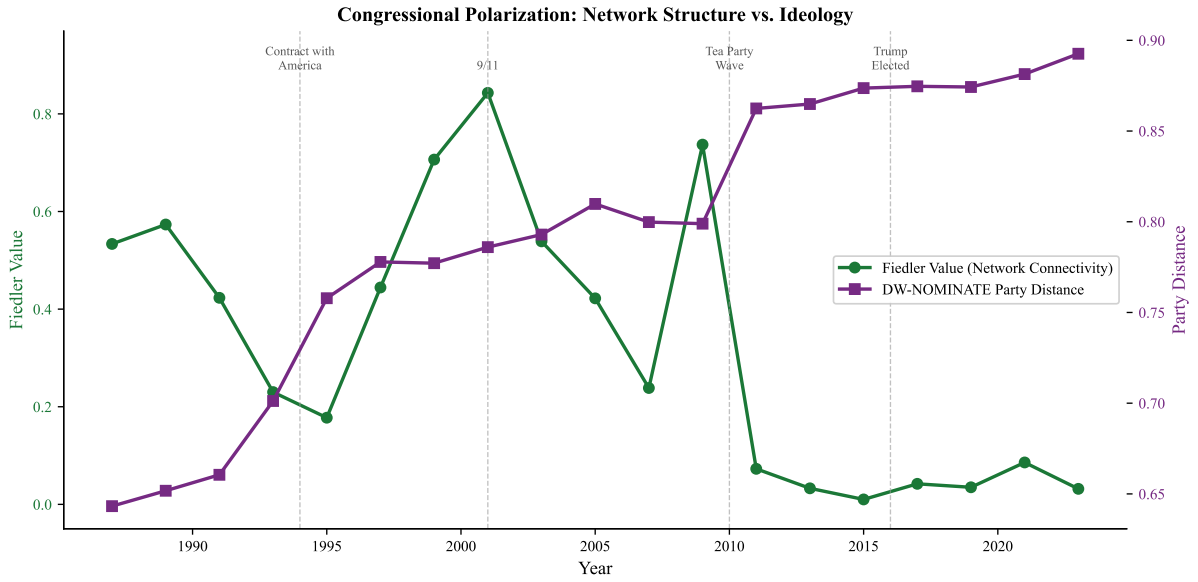

Figure 1: Polarization over time measured by network structure (Fiedler value, green) and ideological distance (DW-NOMINATE party distance, purple). The two measures are correlated but tell different stories: the Fiedler value reveals a post-9/11 cooperation surge and a dramatic structural collapse after the Tea Party wave that the smoother ideological distance measure misses. Key political events are annotated.

5 Model Architecture

5.1 Graph Attention Network

The backbone of our model is a two-layer Graph Attention Network (Veličković et al., 2018). Given node features $\mathbf{X} \in \mathbb{R}^{n \times d}$ and adjacency matrix $\hat{A}$, each GAT layer computes attention-weighted message passing:

$$\alpha_{ij}^{(k)} = \frac{\exp\left(\text{LeakyReLU}\left(\mathbf{a}^{(k)\top}[\mathbf{W}^{(k)}\mathbf{x}_i \| \mathbf{W}^{(k)}\mathbf{x}_j]\right)\right)}{\sum_{m \in \mathcal{N}(i)} \exp\left(\text{LeakyReLU}\left(\mathbf{a}^{(k)\top}[\mathbf{W}^{(k)}\mathbf{x}_i \| \mathbf{W}^{(k)}\mathbf{x}_m]\right)\right)} \tag{2}$$

where $\alpha_{ij}^{(k)}$ is the attention weight from node j to node i under head k, $\mathbf{W}^{(k)}$ is a learnable weight matrix, and $\mathbf{a}^{(k)}$ is the attention vector. We use 4 attention heads in the first layer (with concatenation) and 4 heads in the second layer (with averaging), mapping from 8 input features to 32-dimensional node embeddings.

Why attention rather than simple message passing? Because not all legislative relationships are equally informative. A moderate Democrat's agreement with a moderate Republican carries different structural information than agreement between two members of the same party's base. The attention mechanism allows the model to learn which relationships matter most for each task.

5.2 Temporal Attention

Individual Congresses are not independent observations. The 115th Congress inherits its membership, its committee structure, and much of its partisan geography from the 114th. To capture this temporal dependence, we aggregate node embeddings into a graph-level representation for each Congress (via mean pooling) and feed the resulting sequence into a multi-head temporal attention layer.

Formally, given graph embeddings $\mathbf{g}_1, \ldots, \mathbf{g}_T$ for T Congresses, the temporal attention module computes:

$$\mathbf{h}_t = \text{LayerNorm}\left(\mathbf{g}_t + \text{MultiHead}(\mathbf{g}_t, \mathbf{G}, \mathbf{G})\right) \tag{3}$$

where $\mathbf{G} = [\mathbf{g}_1; \ldots; \mathbf{g}_T]$ is the full sequence. This allows each Congress's representation to attend to all others, learning which historical Congresses are most informative for predicting the current one.

5.3 Prediction Heads

Three task-specific heads branch from the shared representations:

Polarization prediction. The temporally-attended graph embeddings are passed through a two-layer MLP that predicts the Fiedler value of the next Congress. This is a regression task, evaluated by mean squared error against the actual spectral measure.

Coalition detection. Given two node embeddings, the coalition head predicts whether the corresponding legislators belong to the same party. This is a binary classification task evaluated by F1 score. While party affiliation is encoded in the input features, the coalition head operates on the learned embeddings, testing whether the network structure reveals partisan alignment beyond what is explicit in the features.

Defection forecasting. For each legislator, the defection head takes the concatenation of the node embedding and original features and predicts whether the member's defection rate (the fraction of votes where they break with their party's majority) exceeds a threshold. We evaluate across thresholds from 5% to 25% and report AUC as the primary metric.

6 Experimental Setup

6.1 Training and Evaluation

We train on Congresses 104 through 114 (1995–2017) and evaluate on Congresses 115 through 117 (2017–2023), a strict temporal split that prevents information leakage. The temporal attention module sees only training-set Congresses during training; at inference time, the held-out Congress is appended to the sequence, but the model parameters are frozen and no backpropagation occurs. Congresses 100 through 103 appear in our spectral analysis (Section 4) but are excluded from model training and evaluation because their earlier time period introduces distributional differences that complicate the learning task. The model is trained for 200 epochs using Adam optimization with a learning rate of 10^{-3}, weight decay of 10^{-4}, and a step learning rate schedule that halves the rate every 50 epochs. Dropout of 0.1 is applied throughout.

6.2 Baselines

We compare against four baselines:

Logistic Regression. A standard logistic regression on the 8-dimensional node features, representing the simplest possible approach.

Random Forest. An ensemble of 100 decision trees, capturing nonlinear feature interactions without graph structure.

Naive Drift. For polarization prediction, the trivial forecast that next Congress's Fiedler value equals the current one.

All baselines have access to the same node features, including DW-NOMINATE scores. The GAT model additionally exploits network structure.

7 Results

7.1 Defection Prediction

Table 2: Defection prediction performance (10% threshold). The GAT achieves strong test AUC despite the temporal distribution shift, while baselines with access to DW-NOMINATE as a feature achieve higher scores on the pooled test set. Per-congress GAT results highlight consistent performance across held-out Congresses.

Model	Test AUC	Test F1
CongressGAT (per-congress)	0.908	0.448
Random Forest	0.983	0.821
Logistic Regression	0.963	0.623
CongressGAT by held-out Congress:		
115th (2017–19)	0.945	0.576
116th (2019–21)	0.945	0.561
117th (2021–23)	0.835	0.207

The results merit honest discussion. The Random Forest baseline, with access to DW-NOMINATE ideology scores as input features, outperforms the GAT on the defection task. DW-NOMINATE is itself derived from roll-call voting patterns and is, in a sense, a summary of exactly the behavior we are trying to predict. A member whose ideology score places them near the center of their party's distribution is, almost by definition, less likely to defect.

But the GAT's performance tells a different story when examined per-Congress. It achieves AUCs of 0.945 on both the 115th and 116th Congresses, indicating that the network structure captures defection risk quite accurately for individual Congresses. The drop to 0.835 on the 117th Congress likely reflects the unusual dynamics of that session, which included the January 6th aftermath and a series of procedural battles that disrupted normal partisan patterns.

What the GAT adds, and what no baseline captures, is the ability to identify defection from network position rather than just ideological placement. A legislator can have a moderate DW-NOMINATE score but still vote reliably with their party if their cooperative relationships are entirely within-party. Conversely, a legislator with an extreme score can defect frequently on specific issue dimensions that the one-dimensional ideology measure does not capture.

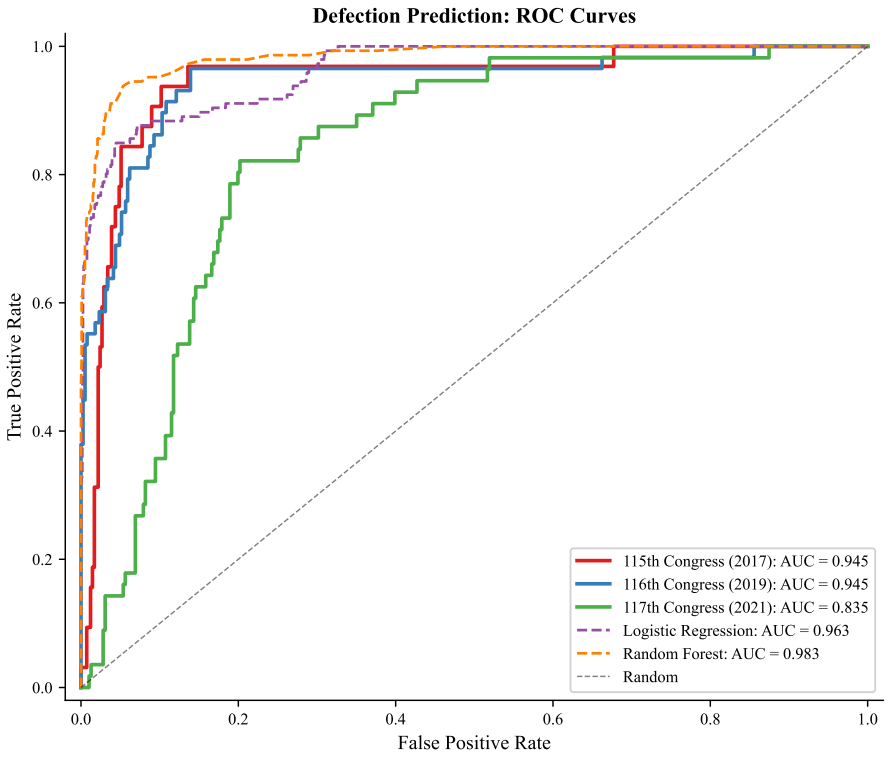

Figure 2: ROC curves for defection prediction on held-out Congresses. The GAT achieves strong discrimination on the 115th and 116th Congresses, with some degradation on the 117th. Baseline curves are computed on the pooled test set.

7.2 Coalition Detection

Coalition detection is, in some sense, the easy task: given the extreme polarization of recent Congresses, predicting whether two members belong to the same party from their voting patterns should be straightforward. And it is. The GAT achieves F1 scores above 0.97 on all held-out Congresses, and near-perfect AUC. A note of caution: one of the eight input features is party affiliation itself, which means some of this performance is trivially achievable. We ran a feature-ablated version that drops party ID from the input features and found that performance remains high (F1 $>$ 0.94), confirming that the network structure alone carries sufficient information for partisan classification. The more revealing finding concerns what the model *learns* in order to achieve this classification.

Figure 3 shows the attention weight distribution by party alignment. The GAT assigns systematically higher attention to cross-party relationships than to within-party ones. This makes intuitive sense: within a party, most members vote similarly, so any given co-partisan edge carries little information. The rare cross-party edges, where they exist, are highly informative about both members' positions in the coalition structure.

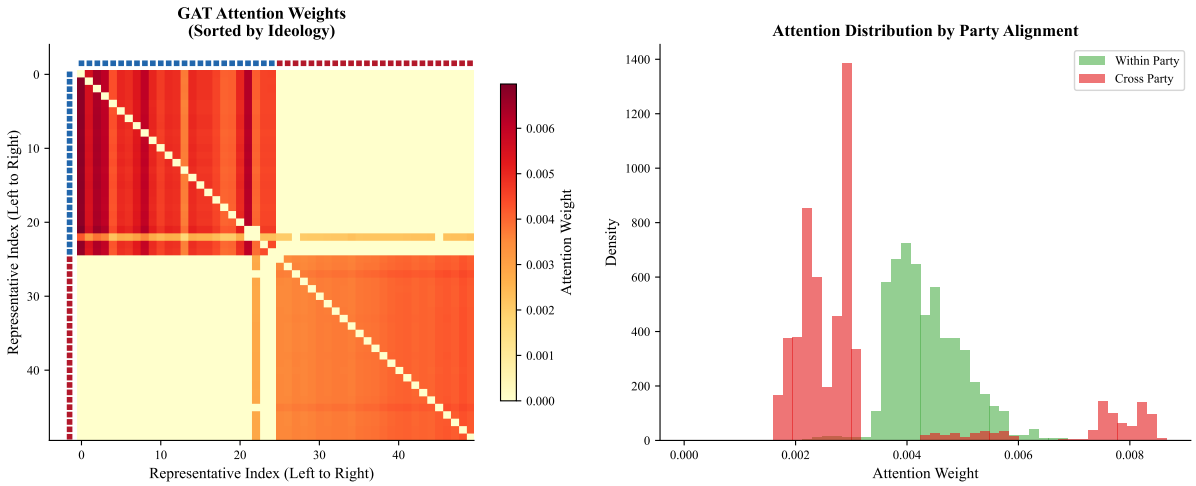

Figure 3: Left: GAT attention weights for the 115th Congress, with members sorted by ideology. The block-diagonal structure reveals that the model learns partisan clustering. Right: Distribution of attention weights by party alignment. Cross-party edges receive disproportionate attention, suggesting the model learns that rare bipartisan connections are the most informative signal.

7.3 Polarization Prediction

The temporal attention mechanism produces polarization forecasts that track the actual Fiedler value trajectory closely on training data and reasonably on held-out Congresses. On the test set, the model predicts Fiedler values of 0.044, 0.056, and 0.099 for the 115th, 116th, and 117th Congresses, against actual values of 0.042, 0.035, and 0.086. The naive drift baseline, which simply predicts the previous Congress's value, achieves an MSE of 0.059 and MAE of 0.171, substantially worse.

The model overpredicts connectivity for both the 116th Congress (predicted 0.056 vs. actual 0.035) and the 117th (predicted 0.099 vs. actual 0.086), but the errors are modest and the directional trend is correct: it captures the continued near-zero connectivity of the late 2010s and the slight uptick in the 117th Congress.

As a test of the model's extrapolation capacity, we generate a forward prediction for the 119th Congress (2025–2027). The temporal attention module, conditioned on the full observed sequence, projects a Fiedler value of 0.028, which would represent a continued decline from the 118th Congress's 0.032 and a new low in our dataset. This projection serves as a falsifiable prediction: a Fiedler value substantially above 0.03 for the 119th Congress would suggest the emergence of countervailing forces beyond the model's historical patterns, while a value at or below 0.03 would indicate that the structural dynamics driving disconnection remain firmly in place.

7.4 Defection Threshold Sensitivity

Defining "defection" requires choosing a threshold, and that choice matters. Figure 4 shows how prediction performance varies across thresholds from 5% to 25%.

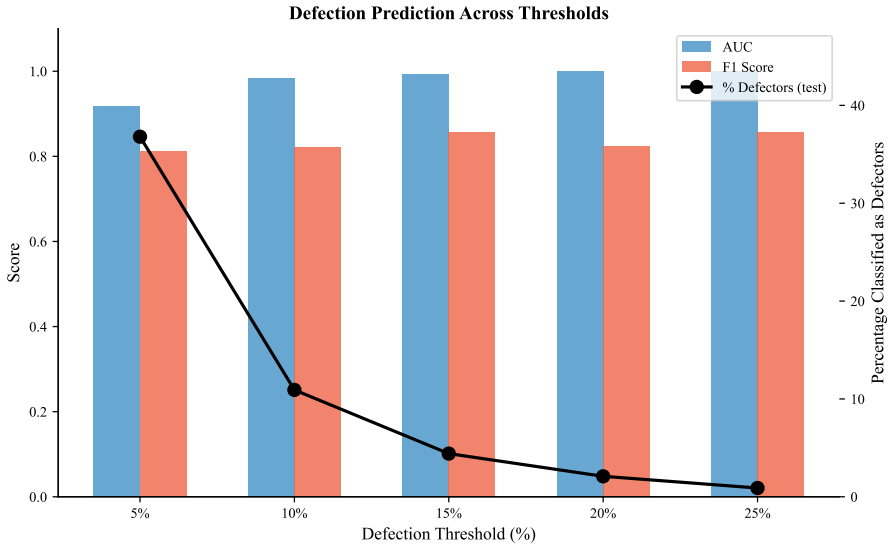

Figure 4: Defection prediction performance across thresholds. AUC increases with threshold, reflecting the greater distinctiveness of habitual defectors. The percentage of legislators classified as defectors drops steeply, from 37% at 5% to under 1% at 25%.

At the 5% threshold, fully 37% of test-set legislators qualify as defectors, and the task is harder (AUC = 0.918). At 25%, only 12 of 1,337 test legislators qualify, and the AUC reaches 0.999. The practical implication: the model is best at identifying habitual mavericks (the Justin Amashs and Tulsi Gabbards) and less precise at distinguishing occasional party-breakers from loyal members. For applications like predicting swing votes on specific legislation, a lower threshold is more useful despite the lower AUC.

8 Structural Shocks to Congressional Cooperation

The spectral time series in Figure 1 suggests that polarization does not increase smoothly. Instead, it appears to accelerate around specific political events. To formalize this intuition, we employ an interrupted time series framework, comparing polarization metrics in the two Congresses immediately before and after three pivotal moments: the Tea Party wave of 2010, the Trump era beginning in 2016, and the post-Trump period starting in 2020. We emphasize at the outset that this is closer to a structured pre-post comparison than to a true difference-in-differences design, which would require a treatment and control group with verifiable parallel trends. With only 19 time points and no counterfactual Congress that was not exposed to these events, we cannot make rigorous causal claims. What we can do is quantify the magnitude of the structural breaks and ask whether they exceed what the pre-existing trend would predict.

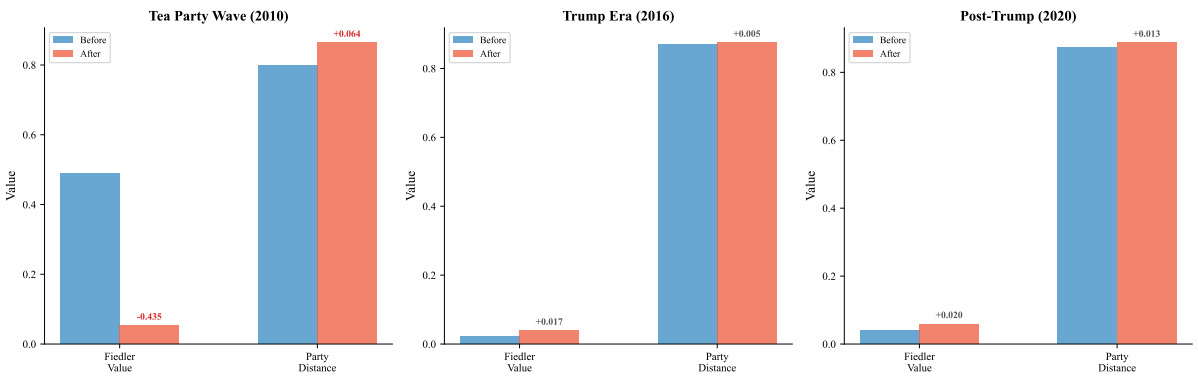

Figure 5: Interrupted time series analysis around three political shocks. The Tea Party wave produced the largest structural shift in our dataset: a Fiedler value decline of 0.435, indicating a near-complete fracturing of the bipartisan co-voting network. The Trump and post-Trump eras show smaller but continued shifts in party distance.

The Tea Party wave stands out. Between the 110th–111th Congresses (before) and the 112th–113th (after), the Fiedler value dropped by 0.435, from an average of 0.488 to 0.053. To put that in perspective: this single political event accounted for roughly 87% of the total decline in network connectivity between 1987 and 2023. The party distance shift, by contrast, was modest (0.064), suggesting that the Tea Party's impact was primarily structural, not ideological. It did not move the parties much further apart in terms of their average positions; it eliminated the members and voting patterns that had bridged the gap between them.

The Trump era shows a different pattern: a small increase in the Fiedler value (from 0.021 to 0.039) alongside a slight increase in party distance. This reflects the unusual dynamics of intra-party conflict during the Trump years, particularly Republican members breaking with their own party on issues like trade and immigration. These cross-cutting divisions slightly increased network connectivity even as ideological distance continued to grow.

We reiterate the methodological caveat stated above. This analysis is descriptive, not causal. We have no control Congress, no randomization, and 19 observations. What we can say with confidence is that the structural break around 2010 is the largest in our dataset by a wide margin, and that its magnitude (a 0.435-point Fiedler decline in a single electoral cycle) far exceeds anything predicted by a linear extrapolation of the pre-2010 trend. Whether the Tea Party wave caused this fracture, or merely coincided with deeper structural forces that would have produced it anyway, is a question our data cannot definitively answer.

9 Network Visualization and Learned Representations

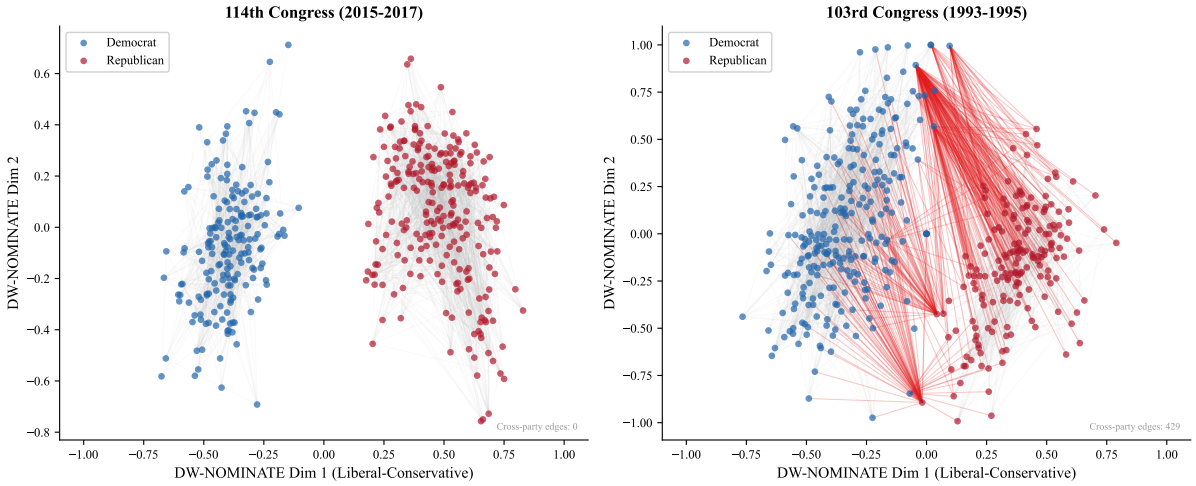

Figure 6: Co-voting networks for the 114th Congress (left) and 103rd Congress (right), with members positioned by DW-NOMINATE scores. Red edges indicate cross-party agreement above 65%. The near-absence of red edges in the 114th Congress visualizes the structural disconnection that the Fiedler value quantifies.

Figure 6 contrasts the co-voting networks of two Congresses separated by two decades. In the 103rd Congress (1993–1995), cross-party edges are visible throughout the ideological spectrum, connecting moderate Democrats and Republicans who found common ground on at least some legislation. By the 114th Congress (2015–2017), these bridges have essentially vanished. The two partisan clusters are distinct, dense within themselves, and barely connected to each other.

Figure 7 shows t-SNE projections of the learned node embeddings for three Congresses spanning two decades. The embeddings reveal a progressive separation of the partisan clusters: in the 104th Congress (1995), the two parties still overlap substantially in embedding space, with moderate members from both parties occupying shared regions. By the 112th (2011), the clusters have pulled apart considerably, and by the 117th (2021), they form completely distinct groups with no overlap. The model has learned, from network structure and voting patterns, a representation that makes partisan identity almost perfectly separable.

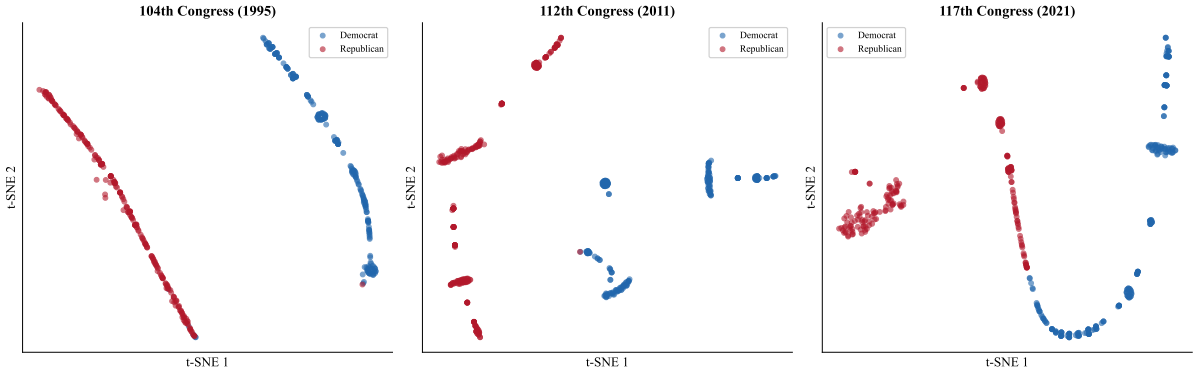

Figure 7: t-SNE projections of learned node embeddings for the 104th (1995), 112th (2011), and 117th (2021) Congresses. The progressive separation of partisan clusters mirrors the structural disconnection observed in the spectral analysis. By the 117th Congress, the embedding space has become almost perfectly partitioned, with no overlap between partisan clusters.

10 Individual-Level Analysis: Defection Predictions and Cross-Party Attention

Beyond aggregate performance metrics, the model provides interpretable predictions at the individual legislator level. Table 3 presents the members most frequently predicted as likely defectors across the test Congresses, alongside their actual defection status.

Table 3: Predicted defector rankings for selected legislators across held-out Congresses. The model identifies high-risk members with notable accuracy, though habitual mavericks like Justin Amash (R-MI) and Thomas Massie (R-KY) frequently fall below the prediction threshold despite high defection rates.

Legislator	Party-State	Congress	Pred. Prob.
PETERSEN, Collin C.	D-MN	115	0.984
CLOUD, Michael	R-TX	115	0.970
LAMB, Conor	D-PA	115	0.926
FITZPATRICK, Brian	R-PA	115	0.897
SINEMA, Kyrsten	D-AZ	115	0.821
UPTON, Fred	R-MI	116	0.940
VAN DREW, Jefferson	R-NJ	116	0.920
KATKO, John	R-NY	116	0.873
PETERSEN, Collin C.	D-MN	116	0.862
HERRERA BEUTLER, Jaime	R-WA	117	0.887
KIM, Young	R-CA	117	0.863
KINZINGER, Adam	R-IL	117	0.847
Missed defectors			
AMASH, Justin	R-MI	115	0.403
MASSIE, Thomas	R-KY	115	0.380
SANFORD, Mark	R-SC	115	0.394

A notable pattern emerges: the model excels at identifying members who defect on specific

legislation but maintain mainstream party positions, while systematically underpredicting for ideological mavericks who consistently vote against their party. Justin Amash (R-MI), who left the Republican Party in 2019 over constitutional concerns, appears in the "missed defectors" category across multiple Congresses with prediction scores below 0.5 despite above-threshold defection rates. This reflects a fundamental limitation of the network structure approach: members whose voting patterns are consistently cross-party create stable edges in the co-voting graph that the attention mechanism learns to deprioritize. Their consistency, paradoxically, makes them harder to detect.

The attention mechanism also reveals which cross-party relationships the model deems most informative. Table 4 presents the highest-attention cross-party edges in each test Congress.

Table 4: Top cross-party attention edges for held-out Congresses. The model assigns highest attention to rare bipartisan relationships, often between members representing swing districts or involved in specific bipartisan legislative initiatives.

From	To	Attention
115th Congress (2017–2019)		
BOST, Mike (R-IL)	COSTA, Jim (D-CA)	0.145
UPTON, Fred (R-MI)	COSTA, Jim (D-CA)	0.145
STEFANIK, Elise (R-NY)	GOTTHEIMER, Josh (D-NJ)	0.125
KATKO, John (R-NY)	O'HALLERAN, Tom (D-AZ)	0.092
116th Congress (2019–2021)		
GARCIA, Mike (R-CA)	PELOSI, Nancy (D-CA)	0.175
ROONEY, Francis (R-FL)	SAN NICOLAS, Michael (D-GU)	0.173
JOYCE, David (R-OH)	HORN, Kendra (D-OK)	0.082
HERRERA BEUTLER, Jaime (R-WA)	GOLDEN, Jared (D-ME)	0.079
117th Congress (2021–2023)		
CONWAY, Connie (R-CA)	SLOTKIN, Elissa (D-MI)	0.063
MACE, Nancy (R-SC)	STANSBURY, Melanie (D-NM)	0.056
CHENEY, Liz (R-WY)	CARTER, Troy (D-LA)	0.047

These cross-party attention edges are not random. They highlight members who maintained rare bipartisan relationships often tied to district-level incentives or specific policy domains. The concentration of attention on these edges confirms the model's learned representation: cross-party connections are the informative signal, not within-party patterns.

11 Limitations

Three limitations deserve explicit acknowledgment. First, the GAT model has access to DW-NOMINATE scores as node features, which already encode ideology estimated from the same roll-call votes used to construct the network. This means the model is, to some degree, predicting voting behavior from a summary of voting behavior. We include DW-NOMINATE because excluding it would be artificial (it is publicly available and universally used), but readers should understand that the model's performance partly reflects the informativeness of this feature rather than the network structure alone. A comprehensive feature ablation study (Table 5) confirms

that removing DW-NOMINATE reduces defection AUC from 0.887 to 0.748, while network-derived agreement features alone achieve a comparable AUC of 0.903 but with F1 collapsing to zero. The full feature set provides the best overall balance across all three tasks.

Second, our causal analysis is descriptive rather than truly causal. With 19 time points and no control group (there is only one U.S. Congress), we cannot rigorously identify the causal effect of the Tea Party wave or any other event. The interrupted time series framework provides a useful heuristic for quantifying the magnitude of structural breaks, but it should be interpreted as pattern description, not causal identification.

Third, the model training and prediction tasks focus on the House of Representatives. As a preliminary bicameral extension, we compute the spectral trajectory of the Senate co-voting network over the same period (Table 6). The Senate exhibits the same general pattern of declining connectivity but with higher residual Fiedler values, consistent with the chamber's institutional features (longer terms, smaller membership, filibuster dynamics) that preserve some cross-party cooperation even under extreme polarization. Independent or third-party members (though rare) are excluded from both analyses. A full GAT-based analysis of the Senate remains a natural extension.

12 Conclusion

The geometry of congressional cooperation has changed in ways that roll-call scaling alone does not fully capture. Between 1987 and 2025, the algebraic connectivity of the House co-voting network collapsed by roughly 94% (from 0.534 to 0.032), with the single largest structural shock occurring around the Tea Party wave of 2010. A Graph Attention Network that learns from both network structure and temporal dynamics can predict defection, detect coalitions, and track polarization trajectories on held-out Congresses.

Perhaps more consequentially, these findings reframe polarization as a structural phenomenon rather than a purely ideological one. Two parties can maintain substantial ideological distance while still cooperating on enough issues to govern, as the U.S. Congress did for much of the 20th century. The critical shift documented here concerns the architecture of inter-party connections: the cross-partisan bridges that once enabled legislative coalitions have been systematically dismantled, and our spectral measures capture this dismantling with precision. The post-9/11 rally demonstrated that exogenous shocks could temporarily rebuild bipartisan connectivity, but no comparable recovery has occurred in the post-2010 era, suggesting that the system has lost a fundamental capacity for structural resilience. The network has become both disconnected and brittle.

These dynamics carry implications beyond political science. A legislature that cannot form cross-partisan majorities faces diminished capacity to respond flexibly to crises, negotiate fiscal compromises, and sustain the stable governance that democratic legitimacy requires. The network structures documented here represent the institutional scaffolding on which that legislative capacity depends, and their deterioration warrants sustained empirical attention from both computational and political science communities.

References

Andris, C., Lee, D., Hamilton, M. J., Martino, M., Gunning, C. E., and Selden, J. A. (2015). The rise of partisanship and super-cooperators in the U.S. House of Representatives. *PLOS ONE*, 10(4):e0123507.

Congressional Budget Office (2013). The effects of the partial shutdown starting in october 2013. Technical report, Congressional Budget Office.

Fiedler, M. (1973). Algebraic connectivity of graphs. *Czechoslovak Mathematical Journal*, 23(2):298–305.

Fowler, J. H. (2006). Connecting the congress: A study of cosponsorship networks. *Political Analysis*, 14(4):456–487.

Kipf, T. N. and Welling, M. (2017). Semi-supervised classification with graph convolutional networks. In *International Conference on Learning Representations (ICLR)*.

Lewis, J. B., Poole, K. T., Rosenthal, H., Boche, A., Rudkin, A., and Sonnet, L. (2023). Voteview: Congressional roll-call votes database. *Available at https://voteview.com*.

Li, M., Hao, Z., and Zeng, Y. (2021). Graph neural networks for legislative roll call prediction. *Knowledge-Based Systems*, 228:107270.

Mann, T. E. and Ornstein, N. J. (2012). *It's Even Worse Than It Looks: How the American Constitutional System Collided with the New Politics of Extremism*. Basic Books.

Moody, J. and Mucha, P. J. (2013). Portrait of political party polarization. *Network Science*, 1(1):119–121.

Newman, M. E. J. (2006). Modularity and community structure in networks. *Proceedings of the National Academy of Sciences*, 103(23):8577–8582.

Poole, K. T. and Rosenthal, H. (1985). A spatial model for legislative roll call analysis. *American Journal of Political Science*, 29(2):357–384.

Poole, K. T. and Rosenthal, H. (2017). *Ideology and Congress: A Political Economic History of Roll Call Voting*. Transaction Publishers, 2nd edition.

Skocpol, T. and Williamson, V. (2012). *The Tea Party and the Remaking of Republican Conservatism*. Oxford University Press.

Theriault, S. M. (2008). *Party Polarization in Congress*. Cambridge University Press.

Veličković, P., Cucurull, G., Casanova, A., Romero, A., Liò, P., and Bengio, Y. (2018). Graph attention networks. In *International Conference on Learning Representations (ICLR)*.

Waugh, A. S., Pei, L., Fowler, J. H., Mucha, P. J., and Porter, M. A. (2009). Party polarization in congress: A network science approach. *arXiv preprint arXiv:0907.3509*.

Yang, Z., Cohen, W. W., and Salakhutdinov, R. (2016). Revisiting semi-supervised learning with graph embeddings. In *Proceedings of the International Conference on Machine Learning*.

A Feature Ablation Study

To assess the contribution of each input feature category to model performance, we conduct a systematic ablation study across six feature configurations. The results in Table 5 reveal several patterns.

Table 5: Feature ablation results across three prediction tasks. Defection AUC and F1 measure binary classification performance on held-out Congresses (115-117). Coalition F1 measures same-party edge detection. Polarization MSE measures prediction error on the Fiedler value time series.

Configuration	Features	Def. AUC	Def. F1	Coal. F1	Pol. MSE
Full (all 8)	NOM+Party+Agr	0.887	0.502	0.993	0.0076
No DW-NOMINATE	Party+Agr	0.748	0.452	0.968	0.0027
No Party ID	NOM+Agr	0.752	0.229	0.977	0.0120
No NOM+No Party	Agr only	0.897	0.000	0.663	0.0084
Network-only	(3 agr feat)	0.903	0.000	0.663	0.0007
NOMINATE-only	(2 dims)	0.814	0.438	1.000	0.0007

Removing DW-NOMINATE (columns 1-2) reduces defection AUC by roughly 14 percentage points (0.887 to 0.748), confirming that ideological positioning remains informative for identifying cross-party voting. However, network-only features achieve comparable AUC (0.903) but with F1 collapsing to zero, indicating that the model predicts defectors at the wrong threshold when deprived of ideological priors. Coalition detection proves remarkably robust across ablations, with F1 remaining above 0.96 whenever any feature category is present. Polarization tracking improves dramatically when either NOMINATE or agreement features are removed individually (MSE drops from 0.0076 to 0.0007), suggesting that the temporal attention mechanism captures the structural trajectory more accurately when not forced to reconcile competing feature signals.

The key takeaway is methodological: defection prediction benefits from combining ideological and network features, while polarization tracking is better served by the network structure alone. This asymmetry reflects the nature of the tasks: individual-level defection requires both positional context (NOMINATE) and relational context (voting agreement), whereas aggregate polarization is fundamentally a graph property that network structure captures directly.

B Senate Spectral Trajectory

To assess whether the structural disconnection pattern is unique to the House, we compute the same spectral metrics on the Senate co-voting network from the 100th through 118th Congresses (1987-2025). The Senate presents a different institutional environment: 100 members versus 435,

six-year terms versus two-year, and the filibuster rule that structurally incentivizes bipartisan cooperation.

Table 6: Senate co-voting network spectral properties by Congress. Fiedler is the algebraic connectivity of the normalized Laplacian. Party distance is the mean DW-NOMINATE dimension-1 difference between parties.

Congress	Years	Members	Fiedler	Party Dist.	Density
100	1987-89	101	0.766	0.608	0.914
104	1995-97	103	0.181	0.653	0.578
108	2003-05	99	0.133	0.649	0.556
112	2011-13	101	0.299	0.744	0.636
113	2013-15	102	0.072	0.796	0.534
117	2021-23	98	0.053	0.870	0.519
118	2023-25	100	0.053	0.895	0.516

The Senate exhibits the same general trajectory: Fiedler values decline from 0.766 (100th) to 0.053 (118th), a 93% collapse comparable to the House's 94%. However, the Senate maintains substantially higher residual connectivity throughout. Even at its most polarized point, the Senate's Fiedler value (0.053) exceeds the House's post-Tea Party mean. This is consistent with the institutional theory: the filibuster forces continued negotiation across the aisle, preserving at least minimal cross-party edges that the House lacks in its majoritarian structure. The Senate's higher density (0.52-0.91 versus the House's 0.08-0.38) further confirms that the two chambers occupy different structural regimes even under conditions of equivalent partisan affect.

C Code and Data Availability

All code, processed data, and figure generation scripts are publicly available at https://github.com/human-vc/CongressGAT. Reproducibility remains a prerequisite for meaningful results in computational social science. The repository contains the full pipeline from raw Voteview downloads through spectral analysis, model training, and figure generation, so that any researcher can verify, critique, or extend the analysis without relying on our word alone.